Systems & Control Transactions

Research Article
Foundations of Computer Aided Process Design (FOCAPD 2024)
Breckenridge, Colorado, USA. July 14-18, 2024
Peer Reviewed Conference Proceeding

PSE PRESS

Techno economical assessment of a low-carbon hydrogen production process using residual biomass gasification and carbon capture.

E.J. Carrillo [a], J. Lizcano-Prada[b], V. Kafaro [a], D. Rodriguez-Vallejo[c], A. Uribe-Rodríguez[d*]

a Research Center for Sustainable Development in Industry and Energy (CIDES), Universidad Industrial de Santander, 680002 Bucaramanga, Colombia
b TIP, Colombia, Km 7 + 400m Anillo vial Palenque, Diagonal Floridablanca No 22-31 - Bodega 11, Floridablanca, Colombia
c Pfizer, Chemical Research Development, Sandwich, CT13 9NJ, United Kingdom.
d Centre for Innovation and Technology Colombian Petroleum Institute, ECOPETROL, 681011 Piedecuesta, Colombia.
* Corresponding Author: ariel.uribe@ecopetrol.com.co.

ABSTRACT

Aiming to mitigate the environmental impact derived from fossil fuels, we propose an integrated carbon capture-biomass gasification process is proposed to produce low-carbon hydrogen as an alternative energy carrier. The process begins with the pre-treatment of empty fruit bunches (EFB), involving grinding, drying, torrefaction, and pelletization. The resulting EFB pellet is then fed into a dual gasifier, followed by a catalytic cracking of tar and water gas shift reaction to produce syngas, aiming to increase its H_2 to CO ratio. Subsequently, we explore two alternatives (DEPG and MEA) for syngas upgrading by removing CO_2. Finally, a PSA system is modeled to obtain H_2 at 99.9% purity. The pre-treatment stage densifies the biomass from an initial composition (%C 46.47, %H 6.22, %O 42.25) to (%C 54.10, %H 6.09, %O 28.67). The dual gasifier operates at 800°C, using steam as a gasifying agent. The resulting syngas has a volume concentration (%CO 20.0, %CO_2 28.2, %H_2 42.2, %CH_4 5.9). Next stages of the process focus on removing the CO_2 and increased H_2 through catalytic reactions from the syngas. Thus, the DEPG carbon capture process can decrease the CO2 concentration to 2.9%, increasing the hydrogen to 95.6% in volume. In contrast, the MEA process reduces the concentration of CO_2 to 5.2% and increases the concentration of H_2 to 93.1%. Moreover, we estimate a levelized costs of hydrogen (LCOH) and carbon capture cost for each method (DEPG and MEA) (LCOC) and CO_2 avoided (LCCA). LCOH: 3.05 USD/kg H_2, LCOC: 92 and 59 USD/t CO_2 and 183 and 119 USD/t CO_2, for DEPG and MEA respectively.

Keywords: Empty fruit bunch, Gasification, Carbon capture, Torrefaction, Pre-treatment.

INTRODUCTION

In recent years, processes that generate clean energy have gained relevance in academia and industry. Due to the growing energy demand, supplied by the oil industry, there has been a constant increase in greenhouse gas emissions. It is estimated that CO_2 emissions generated by industries are in the order of 8 billion tons per year, it is estimated that emissions will reach 10 billion tons per year [1].

For this reason, several countries such as Japan, Australia, Germany, and most of the countries of the European Union have committed to initiating decarbonization processes, in addition to encouraging processes that lead to a circular economy. One of the energy transition strategies consists of the use of hydrogen as an energy carrier [2]. Currently, the demand for hydrogen has undergone a significant increase from $20\ MT$ (million tons) in 1970 to more than $70\ MT$ by 2018 globally. Most of the hydrogen produced, comes from fossil sources with a commercial value of 1 to $3\ USD$ per kg [3].

In the Colombian context, there is a commitment to reduce CO_2 emissions by 51% by 2030 by promoting the production of hydrogen from sustainable sources [4].

The thermochemical processes are one of the most attractive alternatives in the short term to transform biomass or carbonaceous fuel, into energy and chemical products or their building blocks such as syngas. Depending on the oxygen requirements, the operating temperature and the syngas composition, the thermochemical processes can be classified into pyrolysis, gasification, and combustion [5].

Currently, the predominant transformation process for the biomass is the combustion, which accounts for approximately 90% of its worldwide utilization, generating energy ranging from a few megawatts to 100 megawatts [6]. Nevertheless, nowadays, there is a growing interest in the gasification process due to the flexibility to produce syngas, hydrogen, and biogenic carbon dioxide. As reported by the International Energy Agency (IEA) Bioenergy, as of 2020, there are 686 operational gasifiers worldwide, where 272 plants are producing syngas on a large scale, boasting an energy capacity of approximately $200\ GWth$—equivalent to around $200\ MWth$ per installed gasifier[7].

Biomass gasification is challenging due to its high moisture content, high O/C ratio, low bulk density, lower grindability, and heterogeneous nature, these features make it difficult to use biomass as fuel, for that reason is necessary to carry out a pre-treatment. Furthermore, higher tar formation during the gasification of raw biomass increases the downstream cost of gas separation. Pre-treatment of biomass through torrefaction could remove some of these limitations, making biomass a more suitable feedstock for gasification[8].

Carbon capture stands out as a promising technology to mitigate climate change. The integration of biomass gasification and carbon capture lead to negative net carbon emissions and may therefore provide an important technological alternative for meeting current greenhouse gas stabilization targets. To this end, syngas from biomass gasification combined with pre-combustion carbon capture can be used to produce either biofuels or electricity [9].

It is expected that the technological development of biomass gasification processes coupled with CO_2 capture might satisfy the energy demand in such a way that they can be considered as a technical, economic and environmental feasible alternative. It is hoped that research such as the one presented here could contribute to the development of these processes.

PROCESS DESCRIPTION

Feedstock

The palm oil is a well-established industry in Colombia, this level of industrialization is providing a reliable source of raw material for further transformation into bioenergy, biofuels and biohydrogen among others. We select the empty fruit bunch (EFB), which is a residual biomass from the palm oil extraction as raw material for the gasification process. The EFB characterization given by the ultimate and proximal analysis is shown in Table 1. In additionally, we consider that the EFB has a moisture content of 48% by weight, with a particle size distribution of $40\ cm$ in diameter, following a normal distribution with a mean of $8.3\ cm$. The EFB gasification plant has a design capacity of $80\ t/h$. The biomass was modeled as no-conventional solid, using Aspen plus V12, for enthalpy and density are applied HCOALGEN and DCOALIGT correlations respectively, which are taken by the simulation. The HHV value of biomass moisture provided by simulation is compared to literature data [10].

Table 1: Ultimate and proximal analysis.

Ultimate	Value%	Proximate	Value%
C	46.47	Fixed carbon	16.07
H	6.22	Volatile	69.14
O	42.25	Moisture	48.00
S	0.08	Ash	3.86
N	1.12	HHV	18.5 MJ/Kg
Ash	3.86		

PRE-TREATMENT

This stage encompasses biomass grinding, drying, torrefaction, and pelletization processes. We select two fluid packages: SOLIDS for processes related to biomass, and Redlich-Kwong-Soave-Boston-Mathias for gases generated from the burning of gases and liquids resulting from torrefaction reactions.

The main objective of the pre-treatment is to increase the energy density of the biomass. Thus, the particle size distribution, O/C and H/C ratios can be considered as key performance targets of this stage (Figure 1). At the end of the process, $35.7\ T/h$ torrefied pellets of EFB are produced, with a mass yield of $0.44\ Kg$ pellet torrefied EFB/Kg moisture biomass and ratio of energy consumption of $0.16\ KW/Kg$ pellet torrefied EFB.

Grinding

We simulate this process using the correlations provided by Rosin Rammler and Sperling Bennet, which are retrieved from the Aspen plus database.

We define a target of $5\ mm$ as the particle size, which is predicted as a function of the specific power and Bond work index or Hardgrove grindability index (HGI). The first parameter is given by Ruksathamcharoen with a value of $14\ Kwt/t$ [11], and the second one is provided by Montealegre with a value of 12.6 HGI [12]. See the operation unit CRUSHER in the Figure 1.

Dying

We adapt correlations proposed by Han [13]

Table 3: Comparison raw EFB with torrefied pellets of EFB (PTEFB)

Ultimate analysis	Raw EFB	PTEFB	Proximate	Raw EFB	PTEFB
C	46.47	54.10	Fixed carbon	16.07	23.76
H	6.22	6.09	Volatile	69.14	62.14
O	42.25	28.67	Moisture	48.00	5.35
S	0.08	0.11	Ash	3.86	9.43
N	1.12	1.76	HHV[MJ/Kg]	18.5	20.8
Ash	3.86	9.43			

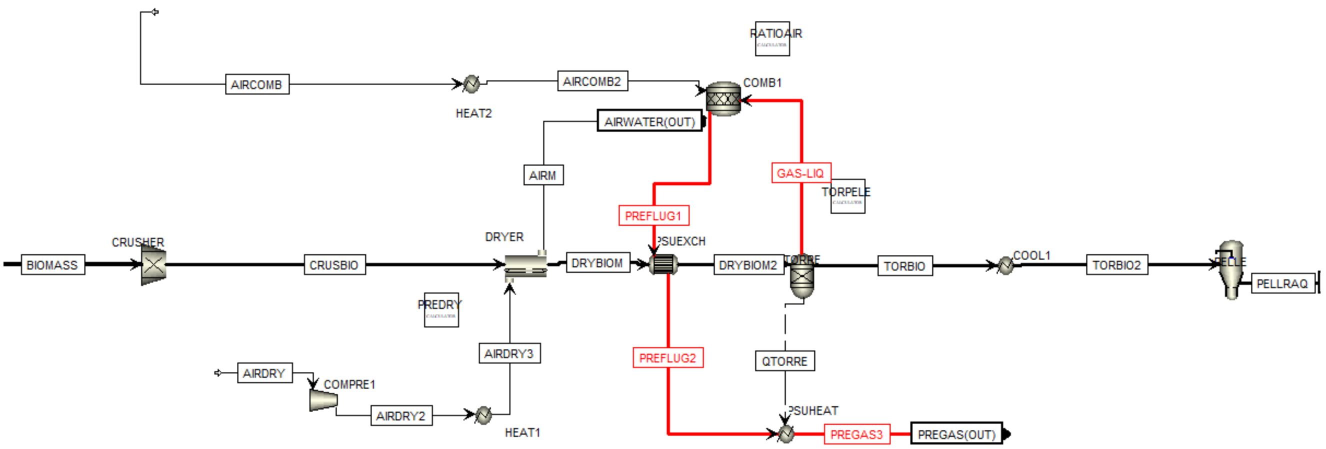

through a CALCULATOR block to predict air demand and sizing for dried This operation unit is represented by the DRYLER, which was set up to operate in co-current. See details in the Table 2.

Table 2: Operations condition and dimensions of DRYLER.

Parameter	value	Units
Length	20.94	m
Cross area	7.02	m^2
Residence time	23	min
Ratio air biomass	7.89	Kg air/Kg EFB
Input air temperature	180	°C
Outlet moisture	9	Weight (%)

Torrefaction

This process seeks to improve O/C and H/C ratios. Thus, the residual biomass can be considered as a vegetal coal, with a performance alike the mineral coal. We represent this operation unit by TORRE and the block calculator TORPELE. We predict yields of solid, liquid and gas and the composition of each phase based on Azir's work [8] [14]. According to the author, the optimum temperature and residence time for the torrefaction process are $250\,^{\circ}C$ and 40 minutes respectively, which are considered in this work (see results in the Table 3). The gas and liquid streams of this process are used to provide the energy requirements for the torrefaction (see red line in Figure 1).

Pelletization

The resulting torrefied EFB is cooled at $100\,^{\circ}C$ before it is fed to the pelletization stage, which is modeled by the GRANULADOR block called PELLE, defining the calculator TORPELLE. It was set up an energy requirement of $30\,Kwt/t$ of EFB to achieve a particle size of $10\,mm$ [15]. Note: The effects of pelletization on the chemical properties of torrefied EFB are not considered.

GASIFICATION

We model a dual gasifier for EFB pellets following the methodology proposed by Puig [16] and Bach [17]. This process operates at atmospheric pressure and using steam as gasification agent. It is selected Peng Robison Boston- Mathias as fluid package for the simulation. In the Figure 2, we represent the gasification process using five blocks (GDES, DEVOL, GH2S-NH3, GOXIR and GREDUCR). The decomposition of torrefied pellets of EFB is modeled by the blocks GDES and DEVOL, using the

Table 4: Mass fractions for each part of the gasification process

Component	Decompositions	Gasification	Combustion chamber
C	0.18	0	0
O_2	0	0	0.04
CO	0.30	0.16	0
CO_2	0.30	0.35	0.24
H_2	0.01	0.03	0
N_2	0.01	0.002	0.70
CH_4	0.04	0.03	0
C_6H_6	0.03	0.01	0
NH_3 (Kg/h)	0	380.5	0
H_2S (Kg/h)	0	29.7	0
C_2H_4	0.07	0	0
H_2O	0	0.42	0
S_2	0.001	0	0
Ash	0.06	0	0.02
Flow rate (T/h)	34.516	59.39	94.50
Stream name	GASCHAR	GAS 10	FLUEG4
Ratio steam/Biomass	0	0.9	0

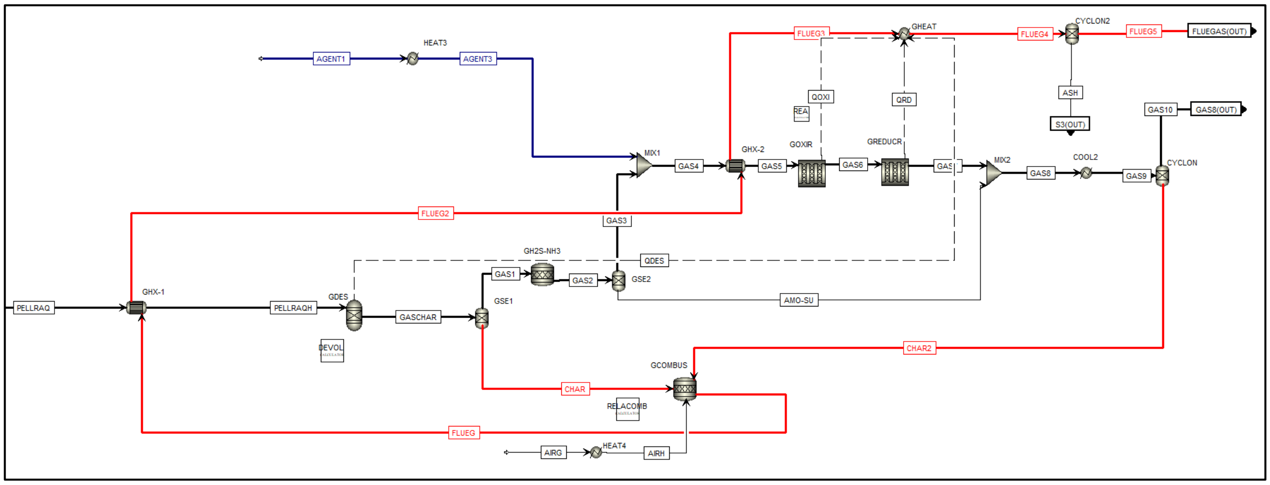

Figure 2. Simulation of dual gasifier.

correlations proposed by Neves [18], which are represented by the equations (1-11). As result, we predict the yield for each component (CO,CO_2,H_2,H_2O, CH_4, C_2H_4,Tar,C, Ash). Note: The operating temperature is the independent variable. According to Lee, the tar fraction is represented as C_6H_6 allowing this assumption to be made[19].

$$\left(\sum_j Y_{j,F} - Y_{ch,F}\sum_j Y_{j,ch}\right) * LHV_G = \left(Y_{tar,F} * Y_{H_2O,F}\right) * LHV_G + Y_{C_2H_4,F} * LHV_{C_2H_4} + Y_{CH_4,F} * LHV_{CH_4} + Y_{CO,F} * LHV_{CO} + Y_{H_2,F}\, LHV_{H_2} \tag{1}$$

$$Y_{ch,F} = 0,106 + 2,43 * e^{(-0,66*10^{-2}*T)} \tag{2}$$

$$Y_{C,ch} = 0,93 + 0,92 * e^{(-0,42*10^{-2}*T)} \tag{3}$$

$$Y_{O,ch} = 0,07 + 0,85 * e^{(-0,48*10^{-2}*T)} \tag{4}$$

$$Y_{H,ch} = -0,41 * 10^{-2} + 0,10 * e^{(-0,24*10^{-2}*T)} \tag{5}$$

$$Y_{H_2,F} = 1,145 * (1 - e^{(-0,11*10^{-2}*T)})^{9,384} \tag{6}$$

$$Y_{CH_4,F} = -2,18 * 10^{-4} + 0,146 * Y_{CO,F} \tag{7}$$

$$Y_{CO,F} = \left(\left(3 * 10^{-4} + \frac{0,0429}{1+\left(\frac{T}{632}\right)^{-7,23}}\right)\right)^{-1} * Y_{H_2,F} \tag{8}$$

$$Y_{C,tar} = 1,14 * Y_{C,bio} \tag{9}$$

$$Y_{O,tar} = 0,8 * Y_{O,bio} \tag{10}$$

$$Y_{H,tar} = 1,13 * Y_{H,bio} \tag{11}$$

The carbon and ashes generated in the decomposition stage are send to a combustion chamber called GCOMBUS, the remaining gas products from decomposition are directed to the stoichiometric reactor called GH2S-NH3, where impurities such as NH_3 and H_2S are formed. These impurities are temporarily separated from the gas, with the aim of excluding them from the gasification reactions and thus maintaining equilibrium. Subsequently, the gas, free of impurities are mixed with steam and enters the gasification stage conducted in the gas reactor, in this case there is not oxygen in the mix, for that reason only the reduced reactions occur, producing a reduced gas. This reduced gas is then mixed with the impurities to obtain synthesis gas. The equations 11-23 represented the reduction reactions.

The red stream in Figure 2 illustrates the energy exchange between the gases generated by the combustion of the solid phase (carbon and ashes) and the chamber of the bubbling bed gasifier. Table 3 displays the mass composition of different stages of the process.

$$C(s) + H_2O \longrightarrow CO + H_2 \tag{12}$$

$$CO + H_2 \longrightarrow C(s) + H_2O \tag{13}$$

$$C(s) + CO_2 \longrightarrow 2CO \tag{14}$$

$$2CO \longrightarrow C(s) + CO_2 \tag{15}$$

$$0{,}5C(s) + H_2 \longrightarrow 0{,}5CH_4 \tag{16}$$

$$0{,}5CH_4 \longrightarrow 0{,}5C(s) + H_2 \tag{17}$$

$$CO + H_2O \longrightarrow CO_2 + H_2 \tag{18}$$

$$CO_2 + H_2 \longrightarrow CO + H_2O \tag{19}$$

$$CH_4 + H_2O \longrightarrow CO + 3H_2 \tag{20}$$

$$CO + 3H_2 \longrightarrow CH_4 + H_2O \tag{21}$$

$$C_6H_6 + 5H_2O \longrightarrow CH_4 + 6H_2 + 5CO \tag{22}$$

$$C_2H_4 + 2H_2O \longrightarrow 2CO + 4H_2 \tag{23}$$

Table 5: Operations condition and dimensions of dual gasifier.

Parameter	value	Units
Temperature gasifier	800	°C
Temperature flue gas	847	°C
Diameter	2.5	m
Length	15	m
Ratio steam biomass	0.9	Kg steam/Kg EFB
Outlet moisture	9	Weight (%)

The proposed model suggests that unreactive char and ash interchange heat with the flue gas as well as syngas thus, temperature of flue gas and solids should be the same. The temperatures of syngas and flue gas are compared with the experimental case. Table 5 shows the operations conditions of gasifier.

The results obtain in the gasification simulation are compared with the experimental data [20]. When comparing the results, errors of less than 15% are observed with respect to the volumetric composition of the products, except for tar, where the error is 20%. These discrepancies arise from differences in the raw materials used, as well as the absence of torrefaction processes in the evaluation performed by Smich. Another significant factor affecting result accuracy is the presence of transfer phenomena, which are not accounted for in the gasifier.

GAS CLEANING AND UPGRATING

Catalytic cracking tar (CCT)

The resulting gas contain quantities of tar (C_6H_6) that can cause tube plugging. However, this tar can also be utilized to enhance the process yield. Therefore, it is crucial to eliminate tar through the catalytic cracking process, as depicted in Figure 3.

The diagram illustrates the necessity to raise the outlet gas temperature to $900\,{}^{\text{o}}C$ to achieve tar destruction using dolomite catalyst (see equation 24), Subsequently gas goes into other catalytic reactor to eliminate methane and transform into CO and H_2 (see equation 25), the final gas contains high concentration of CO, see Table 6. Both reactions follow the Arrhenius model. The kinectic model is provided by Srinivas who investigates [21].

$$C_6H_6 + 2H_2O \longrightarrow 2.5CH_4 + 1.5\text{CO} + 1.5C \tag{24}$$

$$CH_4 + H_2O \longrightarrow CO + 3H_2 \tag{25}$$

Water gas shift reaction (WGSR)

Water gas shift reaction usually occurs in a catalytic environment and high pressures, the reactor operates at 28 bar and the process subdivided into two parts. Hight temperature shift catalytic (HTSC) and Low temperature shift catalytic (LTSC) see the equation (26-27). According to Reza [22] "if high purity of hydrogen is needed, the most common configuration for doing WGSR consist in two consecutive adiabatic fixed bed reactors".

The motive of this arrangement due to the reaction is kinetically favorable at high temperatures while it is thermodynamically at low temperatures. The first reactor used an iron-based catalyst and the second used copper-based catalyst, the Figure 3 shows simulation of

Table 6: Volumetric composition at 0 °C of dry syngas for each process

Component	Gasification	Tar cracking	Methane cracking	HTC	LTC
CO	20.0	20.7	23.0	6.9	1.0
CO_2	28.2	27.4	22.4	32.8	36.5
H_2	44.2	42.9	53.2	59.9	62.1
N_2	0.3	0.3	0.2	0.2	0.2
CH_4	5.9	7.4	0	0	0
C_6H_6	0.0002	0	0	0	0
NH_3 (Kg/h)	380.5	380.5	380.5	380.5	380.5
H_2S (Kg/h)	29.7	29.7	29.7	29.7	29.7
Pressure (bar)	1.0	1.0	1.0	28	25
Temperature (°C)	800	900	900	316	189
Dry flow rate (T/h)	34.516	34.716	36.987	42.884	45.274
Stream name	GAS 11	GAS 12	GAS 13	GAS 26	GAS 28
Reactor volume (m^3)	73.63	1.17	0.20	11.69	2.09

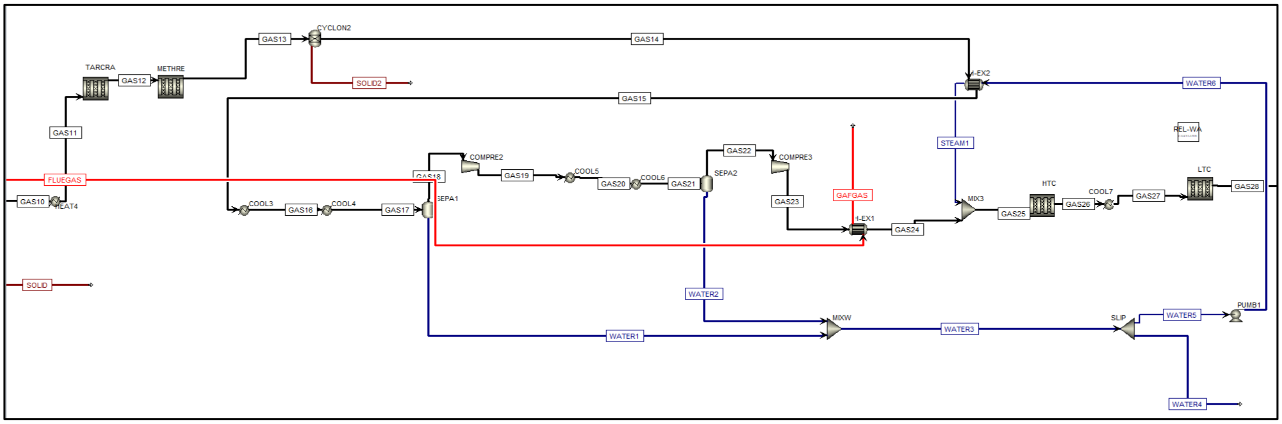

Figure 3. Gas cleaning and upgrading.

each reactor. In the Table 6 shows upgrading gas composition at the end of process.

$$CO + H_2O \leftrightarrow CO_2 + H_2 \tag{26}$$

$$R_{HTSC} = A_C \times 10^{2.845} \exp\left(\frac{-111}{RT}\right) P_{CO} P_{CO_2}^{-0.36} P_{H_2}^{-0.09} \left(1 - \frac{P_{CO_2} P_{H_2}}{K_e P_{CO} P_{H_2O}}\right) \tag{27}$$

$$R_{LTSC} = A_C \times 2.96 \times 10^5 \exp\left(\frac{-47400}{RT}\right) \left(P_{CO} P_{H_2O} - \frac{P_{CO_2} P_{H_2}}{K_e}\right) \tag{28}$$

$$K_e = \exp\left(\frac{-4577.8}{T} - 4.33\right) \tag{29}$$

CARBON CAPTURE

Subsequently, the purified gas, with a high concentration of CO_2 (see Table 6) is directed towards the carbon capture process. In this phase, two alternatives are evaluated based on simulation examples provided by Aspen Plus. Both alternatives employ amines as solvents with the aim of reducing the concentration of components such as CO_2 and H_2S present in the gas stream. For both options, a PSA unit must be installed to achieve hydrogen purity of 99.9%. The simulations presented below correspond to examples extracted from the Aspen Plus V12 database, which were modified for the purified stream in this case [23] [24] .

Physical adsorption

In the first case, DEPG (Dimethyl Ether of Polyethylene Glycol) is employed as the solvent, which eliminates CO_2 through a physisorption mechanism. This system requires high pressure and low temperature. Figure 4 depicts the simulation of the process using DEPG. Table 8 shows the operations conditions.

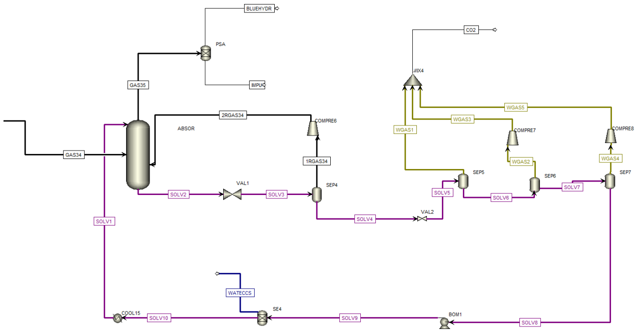

Figure 4. Carbon capture using DEPG as sovent.

Chemical adsorption

For the second case, MEA is used as the solvent. In this system, the interaction occurs through a chemisorption mechanism. Therefore, it is necessary to specify the equilibrium reaction between the solvent and the gas. Figure 5 illustrates the adsorption with MEA. Table 7 shows the results of adsorption for both cases.

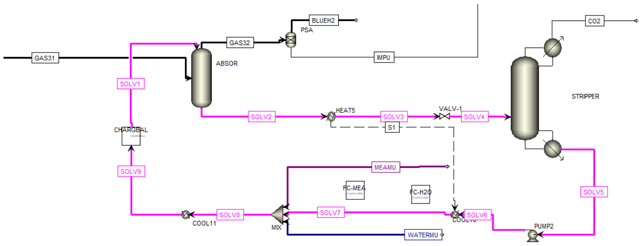

Figure 5. Carbon capture using MEA as sovent.

Table 7: Volume concentration of gas after capture carbon.

Component	DEPG	MEA
CO	1.1	1.4
CO_2	2.9	5.2
H_2	95.6	93.1
N_2	0.3	0.3

Table 8: Operations condition and dimensions of capture processes.

Parameter	DEPG	MEA
Operation temperature (°C)	20	24
Operation pressure (bar)	69	17
Diameter (m)	1.8	1.9
Length (m)	12	3.2
Hydrogen flow rate (T/h)	2.88	3.12
Fluid package	PC-SAFT	ENRTL-RK

It is necessary to mention that although adsorption using MEA results in a higher concentration of hydrogen compared to DEPG (refer to Table 7), there is a loss of hydrogen of 8.9% by weight when using DEPG, while the loss of hydrogen with MEA adsorption is only 1.24%. Subsequently, the gas proceeds to the PSA unit. For DEPG adsorption, it achieves a throughput of $58{,}75\ \frac{Tn}{Day}$ whereas for MEA, it is $63{,}72\ \frac{Tn}{Day}$. The mass yield of MEA and DEPG processes with PSA corresponds to 0.059 and $0.054\ Kg\ hydrogen/kg\ gas$. Additionally, the energy yield is 0.15 and $3.14\ KW\ /Kg\ hydrogen$ respectively.

ECONOMICAL ASSESSMENT

According to the simulation results, economic parameters such as CAPEX and OPEX are calculated using different correlations. For the pre-treatment stage, the methodology proposed by Guthrie [25] is employed. The cost and installation of the dual gasifier are calculated using the correlations presented by Gunnarsson [26]. Two-phase separators are assessed using the methodology proposed by Turton [27], while for the combustion reactor in the pre-treatment and the equipment involved (PSA), the methodology presented by Hoffman [28] is followed.

An interest rate of 11% over a duration of 20 years is assumed, with an estimated construction period of 3 years for the plant.

The economic assessment is conducted separately for each stage of the process (pre-treatment, gasification, and carbon capture).

Pre-treatment

For economic assessment of pre-treatment. We evaluate the LCOE pellets as parameter in the Table 9 shows the results of assessment.

Table 9: Economic assessment of pre-treatment

Parameter	value	Units
CAPEX	$ 2’490.166	USD
OPEX	$ 2’304.759	USD
LCOE pellet	77	$USD/T\ pellet$
Energy consumption	0.120	$MW/T\ pellet$

Gasification and gas upgrading

In the gasification process, we utilize the correlation presented in Gunnarsson [26] for cost estimation. Employing the six-rule method, we estimate the equipment cost and operational expenses using the Lower Heating Value (LHV) of syngas. For the stage of gas cleaning and upgrading, the correlations provided by Warren [25] are applied. The results of the assessment are presented in Tables 10 and 11.

The Levelized Cost of Hydrogen (LCOH) includes costs related to gas cleaning and upgrading. According to GEP company, the LCOH ranges between 2,8 a 3,5 $USD/Kg\ H_2$[29].

Table 10: Economic assessment of gasification

Parameter	value	Units
CAPEX	$ 34’925.863	USD
OPEX	$ 2’327.240	USD
LCOH	3.05	$USD/Kg\ H_2$

Table 11: Economic assessment of gas cleaning and upgrading.

Parameter	value	Units
CAPEX	$ 97.278.973	USD
OPEX	$ 12’726.235	USD

Carbon capture

For the economic assessment, we evaluated both methods of carbon capture. The MEA system was chosen due to its high selectivity to hydrogen compared to the DEPG system. Tables 12 and 13 show the results of the assessment for carbon capture using MEA and DEPG, respectively. In both carbon capture systems, PSA is employed.

The results suggest that the method using DEPG is appropriate, despite its high electricity consumption and low hydrogen production compared to using MEA.

Table 12: Economic assessment of carbon capture using MEA with PSA

Parameter	value	Units
CAPEX	$113’685.286	USD
OPEX	$ 9’682.424	USD
CAPEX/$CO_2\ T/h$	$ 3’062.331	USD
LCOC	92	$USD/T\ CO_2$
LCOA	183	$USD/T\ CO_2$

Table 13: Economic assessment of carbon capture using DEPG with PSA

Parameter	value	Units
CAPEX	$ 83’075.549	USD
OPEX	$ 4’781.573	USD
CAPEX/$CO_2\ T/h$	$ 2’128.205	USD
LCOC	59	$USD/T\ CO_2$
LCOA	119	$USD/T\ CO_2$

CONCLUSION

Based on the process results, it can be affirmed that the proposed model for torrefaction is valid, as it can indirectly estimate the higher calorific value of the torrefied EFB.

It is necessary to clarify that the proposed design does not correspond to the optimum. In the cases of gasification, tar cracking, methane cracking, and water gas shift reaction reactors, sensitivity analysis was conducted to estimate the size of equipment for the base case of carbon capture systems. The simulation extracted from the Aspen Plus examples was modified to consider the resulting flow of the plant proposed in this project.

Regarding gasification, the combination of the models proposed by Puig and Bach, along with the energy integration implemented and Neves' model for the decomposition of the EFB, allows for generating a simulation that emulates the experimental results presented by Schmid, including the formation of tar. In the future, it is considered to consider the reactivity of the ashes.

It is observed that the gas upgrading eliminates most of the problems related to the presence of tar, monoxide, and methane. Additionally, increasing the concentration of hydrogen eliminates problems related to subsequent adsorption, as the presence of tar in the stream can affect the efficiency of adsorption.

The cost of this low-carbon hydrogen is close to the market price. The reasons are related to the high quantities of hydrogen produced in gas upgrading processes WGSR and CCT.

ACKNOWLEDGMENTS

Financial support from the Center for Innovation and Technology Colombian Petroleum Institute (Ecopetrol S.A.) and from the Universidad Industrial de Santander (UIS) for this research project is gratefully acknowledged, as well as the technical support and guide from professionals who are part of the agreement 3042921 between UIS and Ecopetrol. The views expressed in this work do not necessarily reflect those of Ecopetrol S.A.

REFERENCES

1. B. Page and G. Turan, “GLOBAL STATUS OF CCS 2020.” Accessed: Dec. 14, 2023. [Online]. Available: https://www.globalccsinstitute.com/resources/publications-reports-research/global-status-of-ccs-report-2020/#:~:text=The%20Global%20Status%20of%20CCS,over%20the%20past%2012%20months.
2. M. Noussan, P. P. Raimondi, R. Scita, and M. Hafner, “The role of green and blue hydrogen in the energy transition—a technological and geopolitical perspective,” Sustainability (Switzerland), vol. 13, no. 1. MDPI AG, pp. 1–26, Jan. 01, 2021. doi: 10.3390/su13010298.

3. D. Fickling, “Bloomberg. Bloomberg: A Three-Part Series on Hydrogen Energy.” Accessed: Nov. 09, 2023. [Online]. Available: https://www.bloomberg.com/graphics/2020-opinion-hydrogen-green-energy-revolution-challenges-risks-advantages/oil.html
4. Ministerio de ciencias, “Hoja_Ruta_Hidrogeno_Colombia_2810,” 2021.
5. W. J. Martinez-Burgos et al., “Hydrogen: Current advances and patented technologies of its renewable production,” Journal of Cleaner Production, vol. 286. Elsevier Ltd, Mar. 01, 2021. doi: 10.1016/j.jclepro.2020.124970.
6. Irena, “RENEWABLE ENERGY TECHNOLOGIES: COST ANALYSIS SERIES,” 2012. [Online]. Available: www.irena.org/Publications
7. Y. Jafri, L. Waldheim, W. Consulting, and J. Lundgren, Emerging Gasification Technologies for Waste & Biomass. 2020.
8. M. K. Raut, P. Basu, and B. Acharya, “The Effect of Torrefaction Pre-Treatment on the Gasification of Biomass,” International Journal of Renewable Energy & Biofuels, pp. 1–14, Sep. 2016, doi: 10.5171/2016.823723.
9. B. Erlach, B. Harder, and G. Tsatsaronis, “Combined hydrothermal carbonization and gasification of biomass with carbon capture,” Energy, vol. 45, no. 1, pp. 329–338, 2012, doi: 10.1016/j.energy.2012.01.057.
10. S. Krerkkaiwan and D. Boonbumrung, “Production of high quality empty fruit bunch pellet by water washing and torrefaction,” in IOP Conference Series: Earth and Environmental Science, Institute of Physics Publishing, Apr. 2020. doi: 10.1088/1755-1315/463/1/012130.
11. S. Ruksathamcharoen, “EFFECT OF HYDROTHERMAL TREATMENT ON GRINDABILITY AND FUEL CHARACTERISTICS OF EMPTY FRUIT BUNCH DERIVED HYDROCHAR,” pp. 1246–1255, 2018.
12. Montealegre, “Evaluación tecnoeconómica de la torrefacción de biomasa residual de la agroindustria de la palma de aceite en un horno rotatorio,” 2020.
13. J. Han, Y. Choi, and J. Kim, “Development of the Process Model and Optimal Drying Conditions of Biomass Power Plants,” 2020, doi: 10.1021/acsomega.9b03557.
14. M. Azri et al., “A comprehensive study on torrefaction of empty fruit bunches : Characterization of solid , liquid and gas products,” Energy, vol. 230, p. 120877, 2021, doi: 10.1016/j.energy.2021.120877.
15. Vukmirovic, D., & Kokic, B. Effect of steam conditioning on physical properties of pellets and energy consumption in pelleting process. https://www.researchgate.net/publication/277198999
16. M. Puig-gamero, D. T. Pio, L. A. C. Tarelho, and L. Sanchez-silva, “Simulation of biomass gasification in bubbling fluidized bed reactor using aspen plus ®,” vol. 235, no. October 2020, 2021, doi: 10.1016/j.enconman.2021.113981.
17. Q. Bach, D. D. Nguyen, and C. Lee, “Effect of Torrefaction on Steam Gasification of Biomass in Dual Fluidized Bed Reactor — a Process Simulation Study,” pp. 1042–1051, 2019.
18. D. Neves, H. Thunman, A. Matos, L. Tarelho, and A. Gómez-barea, “Characterization and prediction of biomass pyrolysis products,” Prog Energy Combust Sci, vol. 37, no. 5, pp. 611–630, 2011, doi: 10.1016/j.pecs.2011.01.001.
19. S. Y. Lee, T. Alam, J. Kim, J. Lee, and S. Park, “Qualitative analysis of tar based on tar sampling conditions for empty fruit bunch gasification,” 2021.
20. J. C. Schmid, U. Wolfesberger, S. Koppatz, C. Pfeifer, and H. Hofbauer, “Variation of feedstock in a dual fluidized bed steam gasifier-influence on product gas, tar content, and composition,” Environ Prog Sustain Energy, vol. 31, no. 2, pp. 205–215, Jul. 2012, doi: 10.1002/ep.11607.
21. Srinivas, S., Field, R. P., & Herzog, H. J. (2013). Modeling tar handling options in biomass gasification. In Energy and Fuels (Vol. 27, Issue 6, pp. 2859–2873). https://doi.org/10.1021/ef400388u
22. S. R. Janbarari and A. Taheri Najafabadi, “Simulation and optimization of water gas shift process in ammonia plant: Maximizing CO conversion and controlling methanol byproduct,” Int J Hydrogen Energy, vol. 48, no. 64, pp. 25158–25170, Jul. 2023, doi: 10.1016/j.ijhydene.2022.12.355.
23. Aspen Plus. (2021). Aspen Plus example of CO2 capture from syngas for IGCC using DEPG.
24. Aspen Plus b. (2021). Aspen Plus example of CO2 capture from syngas for IGCC using MEA.
25. Warren D., S., Daniel R., L., J. D., S., Soemantri, W., Rafiqul, G., & Ng, K. M. (2016). PRODUCT AND PROCESS DESIGN PRINCIPLES Synthesis, Analysis, and Evaluation (Fourth; WILEY, Ed.). Lightning Source Inc.
26. Gunnarsson, I., Tengberg, F., Thunman, H., Gustavsson, C., & Larsson, A. (2019). Economic assessment of advanced biofuel production via gasification using cost data from the GoBiGas plant. (April 2018), 217–229. https://doi.org/10.1002/ese3.271
27. Turton, R., Shaeiwitz, J. A., & Bhattacharyya, D. (2018). Analysis, Synthesis, and Design of Chemical

Processes (Fifth; Prentice hall, Ed.). Pearson Education, Inc.
28. Hoffman, Z. (2005). LSU Scholarly Repository Simulation and economic evaluation of coal gasification with SETS reforming process for power production
29. GEP. (2023). OUTLOOK FOR GREEN AND BLUE HYDROGEN MARKET. Retrieved from https://www.gep.com/blog/strategy/Green-and-blue-hydrogen-current-levelized-cost-of-production-and-outlook#:~:text=The current levelized cost of blue hydrogen production typically lies,USD 6-11 per MMBtu.
